Rydberg-Atom Terahertz Heterodyne Receiver with Ultrahigh Spectral Resolution

Zhenyue She(佘圳跃)[1,2,3,4†], Xiaojie Zhu(祝孝杰)[5,6†], Yayi Lin(林雅益)[1,2,3,4†], Xianzhe Li(李显喆)[1,2,3,4], Xiaolin Yang(杨小林)[1,2,3,4], Yanfei Shang(尚燕飞)[1,2,3,4], Yuqin Teng(滕玉勤)[1,2,3,4], Haitao Tu(涂海涛)[1,2,3,4], Kaiyu Liao(廖开宇)[1,2,3,4], Caixia Zhang(张彩霞)[1,2,3,4], Xiaohong Liu(刘笑宏)[1,2,3,4*], Jiehua Chen(陈杰华)[5,7,8*], and Wei Huang(黄巍)[1,2,3,4*]

[1]*Key Laboratory of Atomic and Subatomic Structure and Quantum Control (Ministry of Education), School of Physics, South China Normal University, Guangzhou 510006, China*
[2]*Guangdong Provincial Key Laboratory of Quantum Engineering and Quantum Materials, South China Normal University, Guangzhou 510006, China*
[3]*Guangdong-Hong Kong Joint Laboratory of Quantum Matter, Frontier Research Institute for Physics, South China Normal University, Guangzhou 510006, China*
[4]*GPETR Center for Quantum Precision Measurement, South China Normal University, Guangzhou 510006, China*
[5]*State Key Laboratory of Magnetic Resonance and Atomic and Molecular Physics, Innovation Academy for Precision Measurement Science and Technology, Chinese Academy of Sciences, Wuhan 430071, China*
[6]*University of Chinese Academy of Sciences, Beijing 100049, China*
[7]*Key Laboratory of Atomic Frequency Standards, Innovation Academy for Precision Measurement Science and Technology, Chinese Academy of Sciences, Wuhan 430071, China*
[8]*Wuhan Institute of Quantum Technology, Wuhan 430206, China*

(Received 9 April 2024; accepted manuscript online 4 July 2024)

Terahertz heterodyne receivers with high sensitivity and spectral resolution are crucial for various applications. Here, we present a room-temperature atomic terahertz heterodyne receiver that achieves ultrahigh sensitivity and frequency resolution. At a signal frequency of 338.7 GHz, we obtain a sensitivity of $2.88 \pm 0.09\,\mu\text{V}\cdot\text{cm}^{-1}\cdot\text{Hz}^{-1/2}$ for electric field measurements. The calibrated linear dynamical range spans approximately 89 dB, ranging from -110 dBV/cm to -21 dBV/cm. We demodulate a 400 symbol stream encoded in 4-state phase-shift keying, demonstrating excellent phase detection capability. By scanning the frequency of the local oscillator, we realize a terahertz spectrometer with Hz level frequency resolution. This resolution is more than two orders of magnitude higher than that of existing terahertz spectrometers. The demonstrated terahertz heterodyne receiver holds promising potential for working across the entire terahertz spectrum, significantly advancing its practical applications.

DOI: 10.1088/0256-307X/41/8/084201

Heterodyne receivers are of great importance in terahertz (THz) technology. Through converting THz signal into intermediate frequency (IF) of much lower frequency with a local oscillator (LO), a heterodyne receiver can not only make signal processing more convenient by already well-developed electronics or optoelectronics, but also enable the detectors to achieve higher sensitivity and to acquire phase information simultaneously.[1–4] With a tunable LO, the frequency domain THz spectrum analyzer with high spectral resolution can also be realized. Benefiting from these advantages, THz heterodyne receivers are widely applied in various fields, such as THz spectroscopy for astronomy studies[5–7] and gas sensing,[8–10] high-data-rate communications with a broad IF bandwidth,[11–13] imaging or even the passive imaging utilizing thermal radiation for security or biomedicine.[14–16] Moreover, THz frequency domain spectrometers are powerful apparatuses to observe energy band, refractive index, and complex conductivity of thin-film superconductors without breaking up the Cooper pairs.[17–19]

To improve performance of THz heterodyne receivers, many significant works have been carried out. For example, sources for the LO have been well exploited, which include electronic multiplier-chain sources and optical sources, such as heterodyning optical beams and quantum cascade lasers.[20] Schottky diodes, hot electron bolometers, and superconductor-insulator-superconductor mixers are widely used.[21–23] The effective noise equivalent power (NEP) of a Schottky diode mixer can reach the level of several $\text{fWHz}^{-1/2}$. THz detectors based on topological semimetals are also very sensitive to high speed.[24,25] The plasmonic photo-mixer is demonstrated to offer quantum-level sensitivities with spectral resolution around 1 kHz.[26] Significant advancements have re-

†These authors contributed equally to this work.
*Corresponding authors. Email: liuxiaohong@m.scnu.edu.cn; andychen@apm.ac.cn; WeiHuang@m.scnu.edu.cn
© 2024 Chinese Physical Society and IOP Publishing Ltd

cently been made in microwave electrometry using Rydberg atom-based techniques, particularly through the implementation of the electromagnetically induced transparency (EIT) method.[27–33] Additionally, the introduction of atomic heterodyne has significantly enhanced sensitivity and enabled simultaneous phase detection.[34,35]

Rydberg-atom detectors have also demonstrated their sensitivity in THz spectra[36–39] and their ability to perform imaging through conversion of THz signals to optical signals.[40,41] Through spectra of electromagnetically induced transparency (EIT) related transitions between Rydberg states, the atoms can work as a mixer to down convert the frequency of the received signal field into a laser beat note with a LO.[42,43] Since its capability is restricted by the quantum limit in theory, the atomic heterodyne receiver shows promising prospects in many applications. Considering the applications, developing higher sensitivity and spectral resolution THz heterodyne receivers working at room temperature is of challenge, but is highly sought after. Thus, exploring atomic heterodyne receivers in THz spectra seems attractive.

In this work, we demonstrate an atomic THz heterodyne receiver with ultra-high sensitivity and frequency resolution using a room-temperature cesium (Cs) vapor cell. The linear dynamical range and sensitivity of the electric field measurement are calibrated first. In order to demonstrate phase detection ability, the diagram for the symbol stream encoded in the 4-state phase-shift keying (QPSK) is demodulated by the atomic heterodyne receiver. Following this, our experiment shows that the atomic heterodyne receiver can reach very high spectral resolution.

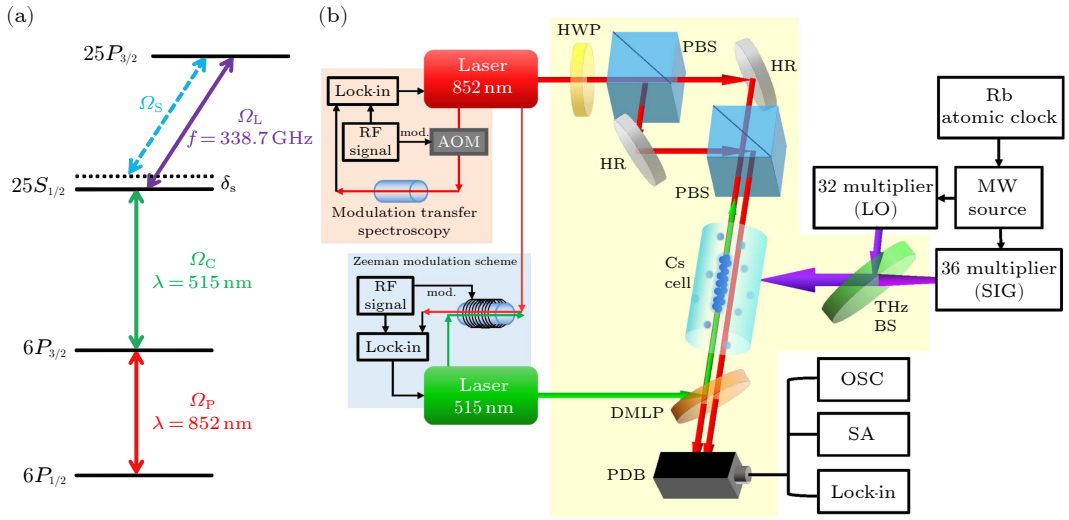

Fig. 1. Energy-level diagram and experimental setup. (a) The Rydberg-atom EIT energy-level diagram of the THz heterodyne receiver. The local THz wave (Ω_L, LO) resonantly drives the Rydberg transition $25S_{1/2} \rightarrow 25P_{3/2}$. The weak THz signal ($\Omega_S$, SIG) also couples this transition with phase ϕ and detuning frequency δ_s relative to the LO field. (b) Experimental setup. The probe and coupling laser beams counter propagate in the cesium (C_S) vapor cell. The 852 nm probe beam (Ω_P) is locked to the $6S_{1/2}(F = 4) \rightarrow 6P_{3/2}(F' = 5)$ transition using modulation transfer spectroscopy, while the 515 nm coupling laser (Ω_C) is locked to the $6P_{3/2} \rightarrow 25S_{1/2}$ transition using the Zeeman modulation scheme. The LO and SIG fields are generated by a 32-times frequency multiplier chain and a 36-times multiplier chain from a two-channel microwave source, respectively. An amplified balanced photo detector (PDB) is used to detect the transmission of probe beam. The data is then analyzed by oscilloscope (OSC), spectrum analyzer (SA) or lock-in amplifier (Lock-in). RF: radio frequency, AOM: acousto-optic modulator, HR: high reflectivity mirror, BS: beam splitter HWP: half-wave plate, PBS: polarization beam splitter, DMLP: dichroic mirror (long pass), MW: microwave.

Experimental Scheme, Linear Dynamical Range and Phase Detection. The Rydberg-atom EIT energy-level diagram of the THz heterodyne receiver is illustrated in Fig. 1. A local THz field (LO) resonantly drives the Rydberg transition $25S_{1/2} \rightarrow 25P_{3/2}$ with a central frequency of 338.7 GHz. The weak signal THz field couples the same transition with phase ϕ_s and detuning frequency δ_s relative to the LO field. The probe and coupling laser beams counter propagate through a room-temperature Cs vapor cell with a length of 5 cm. The 852 nm probe beam is locked to the $6S_{1/2}(F = 4) \rightarrow 6P_{3/2}(F' = 5)$ transition using the modulation transfer spectroscopy.[44] The 515 nm coupling laser is locked to the $6P_{3/2} \rightarrow 25S_{1/2}$ transition using the Zeeman modulation scheme.[45] For the probe beam, the power is 150 μW and the $1/e^2$ beam radius is 150 μm, yielding $\Omega_p/2\pi = 58.58$ MHz. For the coupling beam, the power is 19 mW and the $1/e^2$ beam radius is 75 μm, yielding $\Omega_c/2\pi = 12.89$ MHz. Both the beams pass through a liquid crystal noise eater to minimize the laser amplitude noise. The local THz field and the signal field are generated by frequency multiplier chains from a two-channel microwave source. To facilitate the precise combination of the two THz beams, a THz beam splitter is used. The ratio of transmittance to reflectivity of this beam splitter is about 5.5/4.5. The THz beams are vertically polarized, resulting in a π transition, and the

calculated transition dipole moment is $\mu_{\rm THz} = 242ea_0$. An amplified balanced photo detector (PDB) is used to measure the transmitted probe beam power. The PDB is a commercial product for visible light detection with a bandwidth of 1 MHz. At the optimized point, the change in probe laser transmission $P_{\rm out} = P_{\rm t} - P_0$ is expressed as [34,43]

$$P_{\rm out}(t) = \kappa_0 \Omega_{\rm s} \cos(2\pi\delta_{\rm s} + \varphi_{\rm s}), \tag{1}$$

where the linear expansion coefficient κ_0 depends on the EIT spectrum and LO field $\Omega_{\rm L}$. Then the data from PDB is analyzed by the oscilloscope, spectrum analyzer or lock-in amplifier to acquire parameters of weak THz signal field for different purposes.

As illustrated by the scheme shown in Fig. 1, we experimentally demonstrate a THz heterodyne receiver via room-temperature atomic vapor. The Rydberg atoms are used as a mixer to down convert the THz signal into IF signal with only several hundreds of kHz. For example, with IF frequency $\delta_{\rm s} = 200$ kHz, the linear dynamical range of the IF power as a function of signal electric field is measured by a spectrum analyzer, as shown in Fig. 2(a). To calibrate the entire linear range, we start with two points in the EIT Autler–Townes splitting (ATS) region. The electric fields of the two points can be derived from the equation $E = \hbar\Omega_{\rm THz}/\mu_{\rm THz}$, resulting in the values of 167.72 mV·cm^{-1} and 78.36 mV·cm^{-1}, respectively. Subsequently, the THz power entering the cell is diminished by an 11 dB attenuator. Thus, another two points on the line can be determined precisely. After that, we carefully decrease the microwave power to create electric fields matching the last two points. Then, by using the attenuator again, two more points can be obtained. Step by step, the entire linear range is calibrated. [38,39] The minimum detectable electric field 3.21 ± 0.29 μV/cm (1 s detection time) is acquired when the signal-to-noise ratio (SNR) is 1. The linear dynamical range is 89 dB from −110 dBV/cm to −21 dBV/cm. Furthermore, we measured the sensitivity spectrum of the atomic THz heterodyne receiver as shown in Fig. 2(b). The measured sensitivity S is a function of IF frequency $\delta_{\rm s}$, which is determined by the optical readout noises including PDB and spectrum analyzer, laser noise and transit noise of atoms. From this spectrum, the sensitivity $2.88 \pm 0.09\,\mu$V·cm^{-1}·Hz$^{-1/2}$ with $\delta_{\rm s} = 200$ kHz is realized. The sensitivity derived from the noise spectrum is consistent with the minimum detectable electric field from linear dynamical range calibration.

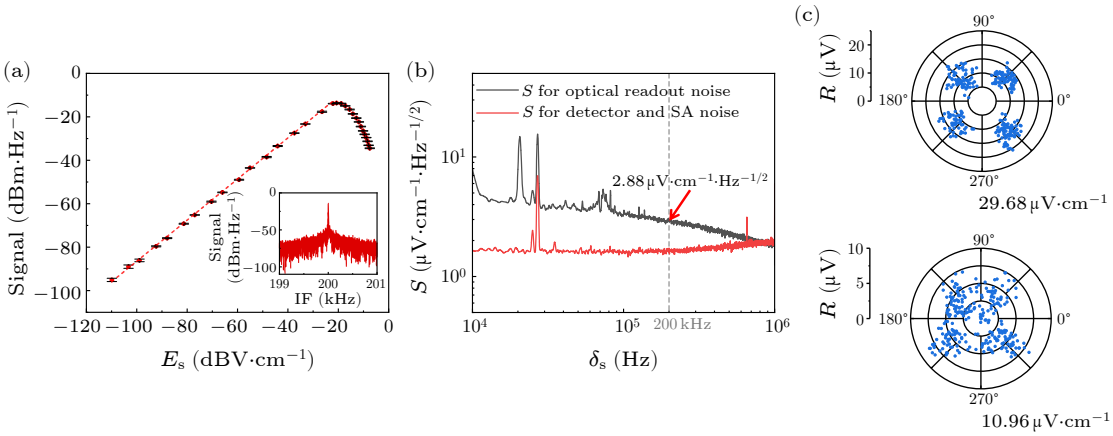

Fig. 2. Linear dynamical range and phase detection. (a) Measured IF power as a function of signal electric field. The error bars indicate standard error from five measurements. The frequency $\delta_{\rm s}$ of IF is 200 kHz. The linear dynamical range is about 89 dB from −110 dBV/cm to −21 dBV/cm. The obtained minimum detectable electric field is 3.21 ± 0.29 μV/cm. (b) Sensitivity spectrum of atomic THz heterodyne receiver. Measured sensitivity S as function of IF frequency $\delta_{\rm s}$. The red solid line shows the total noise from PDB and spectrum analyzer. The sensitivity is determined by the optical readout noises including PDB and spectrum analyzer, laser noise and transit noise of atoms as black solid line shows. At $\delta_{\rm s} = 200$ kHz, the corresponding sensitivity is $2.88 \pm 0.09\,\mu$V·cm^{-1}·Hz$^{-1/2}$. (c) The demodulated QPSK diagrams for 400 symbol stream with modulation frequency 200 kHz. The IF frequency $\delta_{\rm s}$ is 200 kHz. The minimal electric field is 10.96 μV·cm^{-1} when the phase SNR is about 1.

The atomic heterodyne THz receiver also has the capability to accurately measure the phase $\varphi_{\rm s}$. The phase is produced by modulating the fundamental microwave of the THz signal with frequency 200 kHz. Through the 36-times multiplier chain, the phase is magnified by 36 times. Based on this method, the THz signal field is encoded in QPSK. After interacting with the atom vapor, the modulated THz field is phase-sensitive converted into the transmission signal of the probe beam. The modulated signal is monitored by a PDB and then demodulated by a lock-in amplifier. The demodulated QPSK diagrams are shown in Fig. 2(c) for the IF frequency $\delta_{\rm s}$ of 200 kHz. A stream of 400 symbols is recorded in each of the QPSK diagrams. With a large electric field, the four phases can be clearly discriminated. The minimum electric field in our experimental test is 10.96 μV·cm^{-1} when the four phases cannot be distinguished.

THz Spectrometer via Atomic Heterodyne Receiver. A THz spectrometer with very high frequency resolution is also demonstrated using the atomic heterodyne receiver with a multiplier-chain LO source. The measured electric field strength as a function of frequency with a THz

electric field of 40.09 μV·cm^{-1} is shown in Fig. 3(a). From the signal peak at IF frequency $\delta_s = 200$ kHz, the fitted FWHM is 8 Hz. To further verify the frequency resolution, the signal frequency is shifted by ±8 Hz separately. The blue peak corresponds to the +8 Hz frequency shift, while the black peak shows the result of −8 Hz frequency shift. All three peaks can be clearly identified, implying that Hz level frequency precision is achieved.

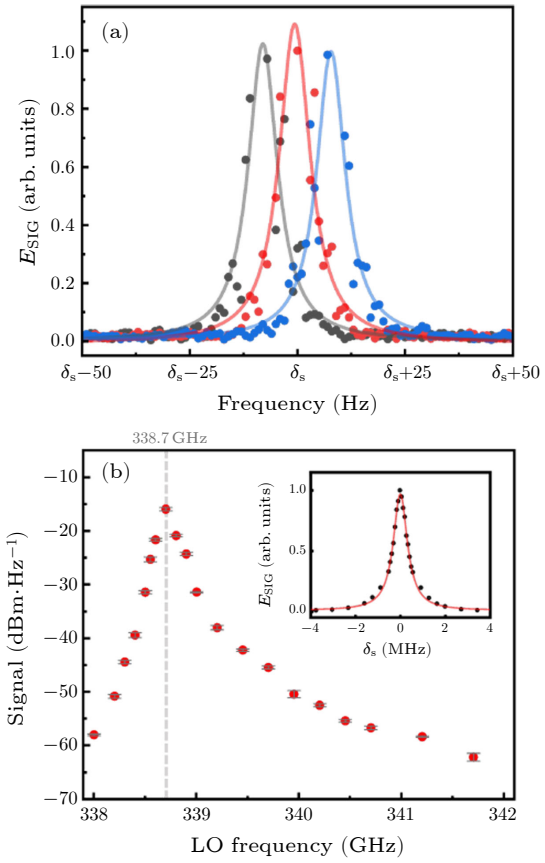

Fig. 3. Atomic THz heterodyne spectrometer. (a) The typical measured signal with about 8 Hz fitted FWHM at IF frequency $\delta_s = 200$ kHz. The blue and black peaks are shifted with ±8 Hz from the center red peak. (b) Measured IF power signal versus LO frequency from 338 GHz to 342 GHz at electric field 92.23 mV·cm^{-1}. The maximum signal intensity is obtained at resonance point marked by the gray dashed line. The inset shows the typical 0.76 MHz instantaneous bandwidth of the THz atomic heterodyne detector measured by scanning the IF frequency with LO frequency 338.7 GHz.

Then we can scan the LO frequency and simultaneously maintain the detuning frequency δ_s equal to 200 kHz. The measured IF power signal as a function of the LO frequency from 338 GHz to 342 GHz at an electric field 92.23 mV·cm^{-1} is shown in Fig. 3(b). The maximum signal −15.9 dBm·Hz^{-1} is obtained at the resonance point marked by the gray dashed line. When deviating from the resonance, the signal strength drops rapidly due to the off-resonance effect.[46] The signal asymmetry is due to the nearby $25P_{1/2}$ state as described in Refs. [43,47]. If simply scan the frequency of THz signal field with LO frequency 338.7 GHz, the bandwidth will be only 0.76 MHz as shown in the inset figure of Fig. 3(b). The calculated linewidth of state $25S_{1/2}$ is about 0.6 MHz, and state $25P_{3/2}$ is 0.2 MHz. Because of the influence such as thermal collision, transit time and other effects, the measured linewidth is deviated from the ideal values.

Discussion. The atomic THz heterodyne receiver demonstrated in the experiment has ultra-high sensitivity and frequency resolution. With the sensitivity achieved in our experiment, the calculated NEP is about 1 fWHz$^{-1/2}$ with effective interaction area 4.72 mm^2. The NEP is better than most room-temperature THz detectors.[14] In addition, the sensitivity and NEP can still be improved. For example, utilizing a split-ring or parallel-plate resonator can increase the sensitivity by two orders of magnitude.[48,49] However, it is important to note that larger frequencies correspond to smaller dipole moments, which ultimately leads to decreasing sensitivity. Additionally, this discrepancy in sensitivity is the primary reason why our results at 338.7 GHz exhibit a considerably lower performance compared to microwave measurement results.[34]

For phase detection, a constant 15° phase noise is presented when increasing the electric field strength. This noise originates from the phase jitter of microwave source and phase deterioration in the frequency multiplier process. Besides the NEP, another significant advantage of the atomic THz heterodyne receiver is the Hz level spectral resolution. This frequency resolution is much better than the previous best record of 1 kHz. The Hz level frequency resolution is not the limit of this heterodyne detector. This resolution is mainly restricted by the SNR obtained from atomic heterodyne detector, also linewidth and phase noise of terahertz sources. To improve the frequency resolution, using microwave sources with lower phase noise to generate terahertz signal and LO is helpful. The increased frequency resolution will provide more details in THz spectroscopy. This will be useful in molecular spectral line recognition, precision measurement of material parameters, and even THz Doppler radar to detect objects with very slow speed. The scanned frequency range in this work is mainly restricted by the THz sources. To utilize a source with a wide enough bandwidth, the frequency range of the atomic receiver can be further expanded by, for example, coupling more Rydberg transitions simultaneously, applying two-photon coupling of off-resonant radio frequencies acting as a tunable LO field, or using spatio-temporal multiplexing of the probe laser.[43,46,50] The atomic heterodyne receiver has the capability to cover the entire THz spectrum.

In conclusion, an atomic THz heterodyne receiver with ultra-high sensitivity and frequency resolution based on a room-temperature cesium (Cs) vapor cell has been demonstrated in our experiment. The linear dynamic range is about 89 dB, from −110 dBV/cm to −21 dBV/cm. The sensitivity of the electric field measurement is 2.88 ± 0.09 μV·cm^{-1}·Hz$^{-1/2}$ with $\delta_s = 200$ kHz at the THz signal frequency of 338.75 GHz. Additionally, phase detection by this atomic heterodyne receiver is attempted, and diagrams for a 400 symbol stream encoded in QPSK are demodulated. Furthermore, the frequency resolution of the

atomic heterodyne receiver can reach Hz, which is significantly better than all existing THz spectrometers. Lastly, a scheme to realize scanning over the entire THz spectrum is proposed.

Acknowledgments. The work was supported by the National Key Research and Development Program of China (Grant No. 2021YFA1402004), the Key-Area Research and Development Program of Guangdong Province, China (Grant Nos. 2019B030330001 and 2020B0301030008), the National Natural Science Foundation of China (Grant Nos. 12225405, 12204182, and U20A2074), and the Innovation Program for Quantum Science and Technology (Grant No. 2021ZD0301705), the Natural Science Foundation of Guangdong Province, China (Grant No. 2022A1515012026).

References

[1] Hübers H W 2008 *IEEE J. Sel. Top. Quantum Electron.* **14** 378
[2] Lin Y J and Jarrahi M 2020 *Rep. Prog. Phys.* **83** 066101
[3] Glaab D, Boppel S, Lisauskas A, Pfeiffer U, Öjefors E, and Roskos H G 2010 *Appl. Phys. Lett.* **96** 042106
[4] Feng W, Zhu Y F, Ding Q F, Zhu K Q, Sun J D, Zhang J F, Li X X, Shangguan Y, Jin L, and Qin H 2022 *Appl. Phys. Lett.* **120** 051103
[5] Neugebauer G, Beichman C A, Soifer B T, Aumann H H, Chester T J, Gautier T N, Gillett F C, Hauser M G, Houck J R, Lonsdale C J, Low F J, and Young E T 1984 *Science* **224** 14
[6] Phillips T G and Keene J 1992 *Proc. IEEE* **80** 1662
[7] Solomon S, Rosenlof K H, Portmann R W, Daniel J S, Davis S M, Sanford T J, and Plattner G K 2010 *Science* **327** 1219
[8] Kloosterman J L, Hayton D J, Ren Y, Kao T Y, Hovenier J N, Gao J R, Klapwijk T M, Hu Q, Walker C K, and Reno J L 2013 *Appl. Phys. Lett.* **102** 011123
[9] Richter H, Buchbender C, Güsten R, Higgins R, Klein B, Stutzki J, Wiesemeyer H, and Hübers H W 2021 *Commun. Earth Environ.* **2** 19
[10] Lin Y J, Cakmakyapan S, Wang N, Lee D, Spearrin M, and Jarrahi M 2019 *Opt. Express* **27** 36838
[11] Koenig S, Lopez-Diaz D, Antes J et al. 2013 *Nat. Photon.* **7** 977
[12] Nagatsuma T, Ducournau G, and Renaud C C 2016 *Nat. Photon.* **10** 371
[13] Ding Q F, Zhu Y F, Xiang L Y, Zhang J F, Li X X, Jin L, Shangguan Y, Sun J D, and Qin H 2023 *Appl. Phys. Express* **16** 024002
[14] Siegel P H and Dengler R J 2006 *Int. J. Infrared Millim. Waves* **27** 465
[15] Siegel P H and Dengler R J 2006 *Int. J. Infrared Millim. Waves* **27** 631
[16] He Y, Liu G, Zhou J, Huang K, Jiang J, and Su W 2022 *Microw. Opt. Technol. Lett.* **64** 1048
[17] Lloyd-Hughes J and Jeon T I 2012 *J. Infrared Millim. Terahertz Waves* **33** 871
[18] Park B C, Kim T H, Sim K I, Kang B, Kim J W, Cho B, Jeong K H, Cho M H, and Kim J H 2015 *Nat. Commun.* **6** 6552
[19] Sherman D, Pracht U S, Gorshunov B, Poran S, Jesudasan J, Chand M, Raychaudhuri P, Swanson M, Trivedi N, Auerbach A, Scheffler M, Frydman A, and Dressel M 2015 *Nat. Phys.* **11** 188
[20] Ren Y, Hovenier J N, Higgins R, Gao J R, Klapwijk T M, Shi S C, Bell A, Klein B, Williams B S, Kumar S, Hu Q, and Reno J L 2010 *Appl. Phys. Lett.* **97** 161105
[21] Crowe T W 1989 *Int. J. Infrared Millim. Waves* **10** 765
[22] Uzawa Y, Wang Z, and Kawakami A 1998 *Appl. Phys. Lett.* **73** 680
[23] Jackson B D, Baryshev A M, de Lange G, Gao J R, Shitov S V, Iosad N N, and Klapwijk T M 2001 *Appl. Phys. Lett.* **79** 436
[24] Hu Z, Zhang L B, Chakraborty A, D'Olimpio G, Fujii J, Ge A P, Zhou Y C, Liu C L, Agarwal A, Vobornik I, Farias D, Kuo C N, Lue C S, Politano A, Wang S W, Hu W D, Chen X S, Lu W, and Wang L 2023 *Adv. Mater.* **35** 2370071
[25] Wang L, Han L, Guo W L, Zhang L B, Yao C Y, Chen Z, Chen Y L, Guo C, Zhang K X, Kuo C N, Lue C S, Politano A, Xing H Z, Jiang M J, Yu X B, Chen X S, and Lu W 2022 *Light Sci. Appl.* **11** 53
[26] Wang N, Cakmakyapan S, Lin Y J, Javadi H, and Jarrahi M 2019 *Nat. Astron.* **3** 977
[27] Sedlacek J A, Schwettmann A, Kübler H, Löw R, Pfau T, and Shaffer J P 2012 *Nat. Phys.* **8** 819
[28] Liao K Y, Tu H T, Yang S Z, Chen C J, Liu X H, Liang J, Zhang X D, Yan H, and Zhu S L 2020 *Phys. Rev. A* **101** 053432
[29] Huang W, Liang Z T, Du Y X, Yan H, and Zhu S L 2015 *Acta Phys. Sin.* **64** 160702 (in Chinese)
[30] Meyer D H, O'Brien C, Fahey D P, Cox K C, and Kunz P D 2021 *Phys. Rev. A* **104** 043103
[31] Cui Y, Jia F D, Hao J H, Wang Y H, Zhou F, Liu X B, Yu Y H, Mei J, Bai J H, Bao Y Y, Hu D, Wang Y, Liu Y, Zhang J, Xie F, and Zhong Z P 2023 *Phys. Rev. A* **107** 043102
[32] Tan C Z, Hu F C, Niu Z J, Jiang Y H, Weidemüller M, and Zhu B 2022 *Chin. Phys. Lett.* **39** 093202
[33] Wang H, Jiao Y, Zhao J, Xiao L, and Jia S 2022 *Chin. Phys. Lett.* **39** 013401
[34] Jing M, Hu Y, Ma J, Zhang H, Zhang L, Xiao L, and Jia S 2020 *Nat. Phys.* **16** 911
[35] Wu F, An Q, Sun Z, and Fu Y 2023 *Phys. Rev. A* **107** 043108
[36] Meyer D H, Castillo Z A, Cox K C, and Kunz P D 2020 *J. Phys. B* **53** 034001
[37] Chen Z W, She Z Y, Liao K Y, Huang W, Yan H, and Zhu S L 2021 *Acta Phys. Sin.* **70** 060702 (in Chinese)
[38] Chen S, Reed D J, MacKellar A R, Downes L A, Almuhawish N F A, Jamieson M J, Adams C S, and Weatherill K J 2022 *Optica* **9** 485
[39] Lin Y Y, She Z Y, Chen Z W, Li X Z, Zhang C X, Liao K Y, Zhang X D, Chen J H, Huang W, Yan H, and Zhu S L 2023 *Fund. Res.* (in press)
[40] Wade C G, Šibalić N, de Melo N R, Kondo J M, Adams C S, and Weatherill K J 2017 *Nat. Photon.* **11** 40
[41] Downes L A, MacKellar A R, Whiting D J, Bourgenot C, Adams C S, and Weatherill K J 2020 *Phys. Rev. X* **10** 011027
[42] Simons M T, Haddab A H, Gordon J A, and Holloway C L 2019 *Appl. Phys. Lett.* **114** 114101
[43] Liu X H, Liao K Y, Zhang Z X, Tu H T, Bian W, Li Z Q, Zheng S Y, Li H H, Huang W, Yan H, and Zhu S L 2022 *Phys. Rev. Appl.* **18** 054003
[44] Preuschoff T, Schlosser M, and Birkl G 2018 *Opt. Express* **26** 24010
[45] Jia F, Zhang J, Zhang L, Wang F, Mei J, Yu Y, Zhong Z, and Xie F 2020 *Appl. Opt.* **59** 2108
[46] Meyer D H,Kunz P D,and Cox K C 2021 *Phys. Rev. Appl.* **15** 014053
[47] Song Z, Liu H, Liu X, Zhang W, Zou H, Zhang J, and Qu J 2019 *Opt. Express* **27** 8848
[48] Holloway C L, Prajapati N, Artusio-Glimpse A B, Berweger S, Simons M T, Kasahara Y, Alù A, and Ziolkowski R W 2022 *Appl. Phys. Lett.* **120** 204001
[49] Wu B, Lin Y, Wu F C, Chen X Z, An Q, Liu Y, and Fu Y Q 2023 *Acta Phys. Sin.* **72** 034204 (in Chinese)
[50] Knarr S H, Bucklew V G, Langston J, Cox K C, Hill J C, Meyer D H, and Drakes J A 2023 arXiv:2302.07316 [quant-ph]